Parametric Rao Test for Multichannel Adaptive Generalized Detector

VYACHESLAV TUZLUKOV
School of Electronics Engineering, College of IT Engineering
Kyungpook National University
1370 Sankyuk-dong Buk-gu Daegu 702-701
SOUTH KOREA
tuzlukov@ee.knu.ac.kr http://spl.knu.ac.kr

Abstract: - The parametric Rao test for multichannel signal detection by the adaptive generalized detector (GD) constructed based on the generalized approach to signal processing in noise is derived by modeling the disturbance signal as a multichannel autoregressive process. The parametric Rao test takes a form identical to that of parametric GD for space-time adaptive processing in airborne surveillance radar systems and other similar applications. The equivalence offers new in-sights into the performance and implementation of the GD. Specifically, the Rao/GD is an asymptotically (in the case of large samples) parametric generalized likelihood ratio test generalized detector (GLRT GD) due to an asymptotic equivalence between the Rao test and the GLRT/ GD. The asymptotic distribution of the Rao/GD test statistic is obtained in the closed form, which follows an exponential distribution under the null hypothesis (the target return signal is absent) and, respectively, a non-central Chi-squared distribution with two degrees of freedom under the alternative hypothesis (the target return signal is present). The noncentrality parameter of noncentral Chi-squared distribution is determined by the output signal-to-interference-plus-noise ratio of a temporal whitening filter. Since the asymptotic distribution at the null hypothesis is independent of the unknown parameters, the Rao/GD asymptotically achieves constant false alarm rate (CFAR) GD. Numerical results show that these results are superior in predicting the performance of the parametric adaptive matched filter even with moderate data support.

Key-Words: - Generalized detector, space-time adaptive processing, multichannel generalized detector, adaptive matched filter, adaptive coherence estimator detector, clutter, jamming.

1 Introduction

Multichannel signal detection is encountered in a wide variety of applications. In radar systems, the sensor arrays are often used to facilitate the so-called space-time adaptive processing, which offers enhanced target discrimination capability compared with space- or time-only processing [1], [2]. In remote sensing systems, the multispectral and hyperspectral sensors are used to collect a spectral information across multiple spectral bands, which can be exploited for classification of different materials or detection of man-made objects on the ground [3], [4]. Other examples of applications include wireless communications, relocation, sonars, audio and speech processing, and seismology [5]–[7].

The multichannel signal detection based on space -time adaptive processing has been successfully used to mitigate the effects of clutter and/or interference in radar, remote sensing, and communication systems [1]–[5]. Traditional detectors based on space-time adaptive processing, including the well-known RMB (Reed, Mallett, and Brennan) detectors [8], Kelly's generalized likelihood ratio test (GLRT) detector [9], the adaptive matched filter (AMF) [10]–[12], the adaptive coherence estimation (ACE) detector [13], [14], and the adaptive generalized detector (AGD) [15]–[17] usually involve estimating and inverting a large-size space-time covariance matrix of the disturbance signal (clutter, jamming, and noise) for each test cell using the target-free training data. This entails high complexity and large training requirement. While the first difficulty may create real-time implementation burdens, the second implies that such covariance matrix based techniques may not be used in heterogeneous (due to varying terrain, high platform altitude, Bistatic geometry, conformal array, among others) or dense-target environment, which offers limited training data.

In the present paper, we modify the adaptive generalized detector (GD) constructed based on the generalized approach to signal processing (GASP) in noise [18]–[23] and apply the parametric Rao test for multichannel signal detection. The idea to employ the generalized detector (GD) for the multichannel radar sensor array has been triggered by the purpose to improve the detection performance of radar sensor systems at the low SNR.

The GD can be considered as a combination of the optimal detector in the Neyman-Pearson (NP) criterion sense and energy detector (ED) [18]–[20]. The main function of GD ED is to detect a signal and the main function of the GD NP is to confirm a detection of the searched signal and to define the detected signal parameters as discussed in detail in [20, Chapter 7, pp. 685–692].

A great difference between the GD ED and conventional ED is a presence of additional linear system, for example, the bandpass filter, at the GD input. This bandpass filter can be considered as the source of additional (reference) noise which does not contain the target return signal from spatially distributed signal source. The GD allows us to formulate a decision statistics about the target return signal presence or absence based on definition of the jointly sufficient statistics of the mean and variance of the likelihood function [20, Chapter 3] while the optimal detectors of classical and modern detection theories make a decision about the target return signal presence or absence based on definition of the mean of the likelihood function, only, and the conventional ED employed by radar sensor array system defines a decision statistics with respect to the target return signal presence or absence based on determination of the variance of the likelihood function only. Thus, an implementation of GD in radar sensor array systems allows us to extract more information from the likelihood function and make a more accurate decision about the target return signal presence or absence in comparison, for example, with the matched filter (MF) or ED.

Theoretically, the GD can be applied to detect any target return signal, i.e. the signal with known or unknown, deterministic or random parameters. The GD implementation in radar and wireless communication is discussed in [23] and [24]–[29], respectively. The signal detection performance improvement using GD in radar sensor system is investigated in [30]–[35]. The first attempt to investigate the GD employment in cognitive radio systems has been discussed in [36].

Addressing the above issues has become an important topic in recent multichannel signal detection research. One effective way to reduce the computational and training requirement is to utilize a suitable parametric model for the disturbance signal and exploit the model of signal detection. For example, the multichannel autoregressive (AR) models have been found to be very effective in representing the spatial and temporal correlation of the disturbance [37]–[40].

Parametric GD (PGD) based on a multichannel AR model is developed here. The PGD has been shown to significantly outperform the aforementioned covariance matrix based detectors for small training size at reduced complexity.Specifically the PGD detector models a disturbance as a multichannel AR process driven by a temporally white but spatially coloured multichannel noise. While traditional space-time adaptive processing detectors perform joint space-time whitening using an estimate of the space-time covariance matrix, the PGD detector adopts a two-step approach that involves temporal whitening via an inverse moving-average (MA) filter followed by spatial whitening.

The parameters that need to be estimated are the AR coefficient matrices and the spatial covariance matrix of the driving multichannel noise, which are significantly fewer than what are involved in estimating the space-time covariance matrix. This is the essence behind the training and computational efficiency of the PGD detector.

The PGD detector was obtained in a heuristic approach by modifying the AGD test statistic. Specifically, it replaces the joint space-time whitening incurred by the AGD detector with two separate whitening procedures in time and space. The test threshold and the false alarm and detection probabilities were determined primarily by computer simulation, due to limited analysis available for the PGD detector.

In the present paper, we apply the parametric Rao test for multichannel signal detection based on the GASP [18]–[23], or in another words, the PGD. The generic Rao test is known to offer a standard solution to a class of parametric testing problems. It is easier to derive and implement than the GLRT GD, and is also asymptotically, large-sample in the number of temporal observations and/or training signals, equivalent to the latter.

The Rao test was used to develop detectors for several other problems [41], [42]. Our parametric Rao/GD differs from the generic one for multichannel signal detection in that we make explicit use of a multichannel AR model for the disturbance signal. We show that the parametric Rao/GD takes a form identical to that of the PGD detector. The only difference is that we use a maximum likelihood (ML) based estimator that involves using both the test and training signals for parameter estimation, whereas the estimators in [38] use only the training signals for parameter estimation. If the ML estimator is utilized, the parametric Rao/GD is asymptotically a parametric GLRT GD.

Under the conditions stated in Section 2, the asymptotic distribution of the test statistic under both hypotheses is obtained in the closed form, which can be used to set the test threshold and compute the

corresponding detection and false alarm probabilities. Since the asymptotic distribution under the hypothesis H_0 is independent of the unknown parameters, the parametric Rao/GD outperforms asymptotically the matched filter (MF). The presented numerical results demonstrate that our asymptotic observations are accurate in predicting the performance of the Rao/GD even when the data size is modest.

The reminder of this paper is organized as following. Section II presents a brief description of the general GD flowchart and the main functioning principles and decision statistics obtained at the GD output. The data model is delivered in Section III. Several types of a priori solutions in the form of the MF, AMF, GLRT, Kelly CFAR detectors are discussed in Section IV. Parametric Rao/GD test with the test statistics and asymptotic analysis are presented in Section V. Detection performance of the MF and AMF are discussed in Section VI for comparative analysis with the detection performance of the PGD. Numerical results obtained under simulation are presented and discussed in Section VII. Finally, the conclusion remarks are made in Section VIII.

2 Conventional GD

As we mentioned before, the GD is constructed in accordance with GASP in noise [18]–[20].GASP introduces an additional noise source that does not carry any information about the incoming target return signal with the purpose to improve the signal processing system performance. This additional noise can be considered as the reference noise without any information about the signal to be detected. The jointly sufficient statistics of the mean and variance of the likelihood function is obtained under GASP employment, while the classical and modern signal processing theories can deliver only a sufficient statistics of the mean or variance of the likelihood function. Thus, GASP implementation allows us to obtain more information about the target return signal incoming at the GD input. Owing to this fact, the detectors constructed on the GASP technology are able to improve the signal detection performance in comparison with other conventional detectors.

The GD consists of three channels (see Fig. 1): the GD correlation detector channel (GD CD) – the preliminary filter (PF), the multipliers 1 and 2, the model signal generator (MSG); the GD autocorrelation channel (GD ED) – the PF, the additional filter (AF), the multipliers 3 and 4, the summator 1; and the GD compensation channel (GD CC) – the summators 2 and 3, the accumulator 1. The threshold apparatus (THRA) device defines the GR threshold.

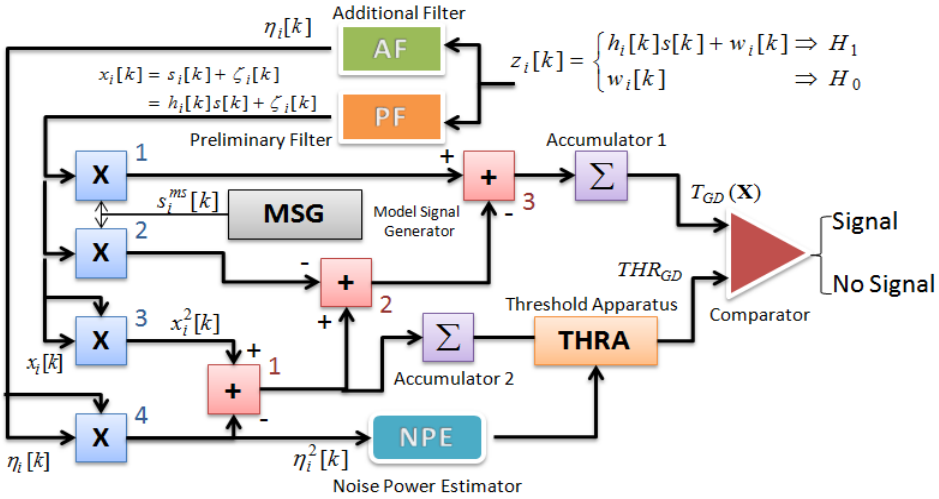

Figure 1. GD structure.

As we can see from Fig. 1, there are two bandpass filters, i.e. the linear systems, at the GR input, namely, the PF and AF. We assume for simplicity that these two filters or linear systems have the same amplitude-frequency characteristics or impulse responses. The AF central frequency is detuned relative to the PF central frequency. There is a need to note the PF bandwidth is matched with the bandwidth of the radio channel or target return signal bandwidth.

If the detuning value between the PF and AF central frequencies is more than 4 or 5 times the target return signal bandwidth to be detected, i.e. $4 \sim 5\,\Delta f_s$, where Δf_s is the target return signal bandwidth, we can believe that the processes at the PF and AF outputs are uncorrelated because the coefficient of correlation between them is negligible (not more than

0.05). This fact was confirmed experimentally in [43] and [44]. Thus, the target return signal plus noise can be appeared at the GR PF output and the noise only is appeared at the GR AF output.

The stochastic processes at the AF and PF outputs present the input stochastic samples from two independent frequency-time regions. If the discrete-time noise $w_i[k]$ at the PF and AF inputs is Gaussian, the discrete-time noise $\xi_i[k]$ at the PF output is Gaussian and the reference discrete-time noise $\eta_i[k]$ at the AF output is Gaussian, too, owing to the fact that the PF and AF are the linear systems and we believe that these linear systems do not change the statistical parameters of the input process. Thus, the AF can be considered as a generator of the reference noise with a priori information a "no" target return signal (the reference noise sample) [21, Chapter 5]. The noise at the PF and AF outputs can be presented in the following form:

$$\begin{cases} \xi_i[k] = \sum\limits_{m=-\infty}^{\infty} g_{PF}[m] w_i[k-m] \ ; \\ \eta_i[k] = \sum\limits_{m=-\infty}^{\infty} g_{AF}[m] w_i[k-m] \ , \end{cases} \tag{1}$$

where $g_{PF}[m]$ and $g_{AF}[m]$ are the impulse responses of the PF and AF, respectively.

In a general, under practical implementation of any detector in radar system with sensor array, the bandwidth of the spectrum to be sensed is defined. Thus, the AF bandwidth and central frequency can be assigned, too (the AF bandwidth can not be used by the target return signal because it is out of its spectrum). The case when there are interfering signals within the AF bandwidth, the action of this interference on the GR detection performance, and the case of non-ideal condition when the noise at the PF and AF outputs is not the same by statistical parameters are discussed in [32].

Under the hypothesis H_1 ("a yes" target return signal), the GR CD generates the signal component $s_i^{ms}[k]s_i[k]$ caused by interaction between the model signal $s_i^{ms}[k]$, the MSG output, and the incoming target return signal $s_i[k]$, and the noise component $s_i^{ms}[k]\xi_i[k]$ caused by interaction between the model signal $s_i^{ms}[k]$ and the noise $\xi_i[k]$ at the PF output. GR ED generates the signal energy $s_i^2[k]$ and the random component $s_i[k]\xi_i[k]$ caused by interaction between the target return signal $s_i[k]$ and the noise $\xi_i[k]$ at the PF output. The main purpose of the GR CC is to cancel completely in the statistical sense the GR CD noise component $s_i^{ms}[k]\xi_i[k]$ and the GR ED random component $s_i[k]\xi_i[k]$ based on the same nature of the noise $\xi_i[k]$. The relation between the target return signal to be detected $s_i[k]$ and the model signal $s_i^{ms}[k]$ is defined as:

$$s_i^{ms}[k] = \mu s_i[k] \ , \tag{2}$$

where μ is the coefficient of proportionality.

The main functioning condition under the GR employment in any signal processing system including the radar sensor one is the equality between parameters of the model signal $s_i^{ms}[k]$ and the incoming target return signal $s_i[k]$, for example, by amplitude. Under this condition it is possible to cancel completely in the statistical sense the noise component $s_i^{ms}[k]\xi_i[k]$ of the GR CD and the random component $s_i[k]\xi_i[k]$ of the GR ED. Satisfying the GR main functioning condition given by (2), $s_i^{ms}[k] = s_i[k]$, $\mu = 1$, we are able to detect the target return signal with the high probability of detection at the low *SNR* and define the target return signal parameters with high accuracy. Practical realization of this condition requires increasing in the complexity of GR structure and, consequently, leads us to increasing in computation cost. For example, there is a need to employ the amplitude tracking system or to use the off-line data samples processing. Under the hypothesis H_0 ("a no" target return signal), satisfying the main GR functioning condition $s_i^{ms}[k] = s_i[k]$ we obtain only the background noise $\eta_i^2[k] - \xi_i^2[k]$ at the GR output.

Under practical implementation, the real structure of GR depends on specificity of signal processing systems and their applications, for example, the radar sensors systems, adaptive communications systems, cognitive radio systems, satellite communication systems, mobile communication systems and so on. In the present paper, the GR circuitry (Fig. 1) is demonstrated with the purpose to explain the main operational principles. Because of this, the GR flowchart presented in the paper should be considered under this viewpoint. Satisfying the GR main functioning condition $s_i^m[k] = s_i[k]$, the ideal case, for radar sensor applications we are able to detect the target return signal with high probability of detection and define accurately its parameters.

In the present paper, we discuss the GR implementation in radar sensor array systems. Since the presented GR test statistics is defined by the signal energy and noise power, see Eq.(3), the equality bet-

ween the model signal $s_i^m[k]$ and the target return signal to be detected $s_i[k]$, in particular by amplitude, is required that leads us to high circuitry complexity in practice. For example, there is a need to employ the amplitude tracking system or off-line data sample processing. Detailed discussion about the main GR functioning principles if there is no a priori information about the target return signal and there is uncertainty with respect to the target return signal parameters, i.e., the target return signal parameters are random, can be found in [18] and [20, Chapter 6, pp.611–621 and Chapter 7, pp. 631–695].

The complete matching between the model signal $s_i^{ms}[k]$ and the incoming target return signal $s_i[k]$ for example, by amplitude is a very hard problem in practice because the incoming target return signal $s_i[k]$ depends on both the fading and the transmitted signal and it is impractical to estimate the fading gain at the low *SNR*. This matching is possible in the ideal case only. The GD detection performance will be deteriorated under mismatching in parameters between the model signal $s_i^{ms}[k]$ and the incoming target return signal $s_i[k]$ and the impact of this problem is discussed in [45], where a complete analysis about the violation of the main GR functioning requirements is presented. The GR decision statistics requires an estimation of the noise variance σ_η^2 using the reference noise $\eta_i[k]$ at the AF output.

Under the hypothesis H_1, the signal at the PF output, see Fig. 1, can be defined as

$$x_i[k] = s_i[k] + \xi_i[k] \ , \tag{3}$$

where $\xi_i[k]$ is the noise at the PF output and

$$s_i[k] = h_i[k]s[k] , \tag{4}$$

where $h_i[k]$ are the channel coefficients. Under the hypothesis H_0 and for all *i* and *k*, the process $x_i[k] = \xi_i[k]$ at the PF output is subjected to the complex Gaussian distribution and can be considered as the independent and identically distributed (i.i.d.) process.

In ideal case, we can think that the signal at the AF output is the reference noise $\eta_i[k]$ with the same statistical parameters as the noise $\xi_i[k]$. In practice, there is a difference between the statistical parameters of the noise $\eta_i[k]$ and $\xi_i[k]$. How this difference impacts on the GR detection performance is discussed in detail in [20, Chapter 7, pp. 631-695].

The decision statistics at the GR output presented in [18] and [20, Chapter 3] is extended for the case of antenna array when an adoption of multiple antennas and antenna arrays is effective to mitigate the negative attenuation and fading effects. The GR decision statistics can be presented in the following form:

$$T_{GR}(\mathbf{X}) = \sum_{k=0}^{N-1}\sum_{i=1}^{M} 2x_i[k]s_i^{ms}[k] - \sum_{k=0}^{N-1}\sum_{i=1}^{M} x_i^2[k] + \sum_{k=0}^{N-1}\sum_{i=1}^{M}\eta_i^2[k] \underset{H_0}{\overset{H_1}{\gtrless}} THR_{GR} \ , \tag{5}$$

where

$$\mathbf{X} = \left[\mathbf{x}(0),...,\mathbf{x}(N-1)\right] \tag{6}$$

is the vector of the random process at the PF output and THR_{GR} is the GR detection threshold.

Under the hypotheses H_1 and H_0 and when the amplitude of the incoming target return signal is equal to the amplitude of the model signal, $s_i^{ms}[k] = s_i[k]$ the GR decision statistics $T_{GD}(\mathbf{X})$ takes the following form, respectively:

$$\begin{cases} H_1 : T_{GD}(\mathbf{X}) = \sum_{k=0}^{N-1}\sum_{i=1}^{M} s_i^2[k] \\ \qquad\qquad + \sum_{k=0}^{N-1}\sum_{i=1}^{M}\eta_i^2[k] - \sum_{k=0}^{N-1}\sum_{i=1}^{M}\zeta_i^2[k] \ , \\ H_0 : T_{GD}(\mathbf{X}) = \sum_{k=0}^{N-1}\sum_{i=1}^{M}\eta_i^2[k] - \sum_{k=0}^{N-1}\sum_{i=1}^{M}\zeta_i^2[k] \ . \end{cases} \tag{7}$$

In (7) the term $\sum_{k=0}^{N-1}\sum_{i=1}^{M} s_i^2[k] = E_s$ corresponds to the average target return signal energy, and the term $\sum_{k=0}^{N-1}\sum_{i=1}^{M}\eta_i^2[k] - \sum_{k=0}^{N-1}\sum_{i=1}^{M}\xi_i^2[k]$ is the background noise at the GR output. The GR output background noise is a difference between the noise power at the PF and AF outputs. Practical implementation of the GR decision statistics requires an estimation of the noise variance σ_η^2 using the reference noise $\eta_i[k]$ at the AF output.

3 Data Model

The problem under consideration involves detecting a known multichannel signal with unknown amplitude in the presence of spatially and temporally correlated disturbance

$$\begin{cases} H_0 : \quad \mathbf{X}_0(n) = \mathbf{D}(n), & n = 0,1,\ldots,N-1 \\ H_1 : \quad \mathbf{X}_0(n) = \alpha\mathbf{S}(n) + \mathbf{D}(n), & n = 0,1,\ldots,N-1 \end{cases} \tag{8}$$

where all vectors are $J \times 1$ vectors, *J* denotes the nu-

mber of spatial channels, and N is the number of temporal observations. Henceforth, $\mathbf{X}_0(n)$ is called the test signal, $\mathbf{S}(n)$ is the signal to be detected with amplitude α, and $\mathbf{D}(n)$ is the disturbance signal that may be correlated in space and time. In addition to the test signal, it is assumed that a set of target-free training or secondary data vectors $\mathbf{X}_k(n), k = 1,2,\ldots,K$ and $n = 0,1,\ldots,N-1$, are available to assist the signal detection.

Define the following $JN \times 1$ space-time vectors:

$$\begin{cases} \mathbf{S} = [\mathbf{S}^T(0), \mathbf{S}^T(1), \ldots, \mathbf{S}^T(N-1)]^T; \\ \mathbf{D} = [\mathbf{D}^T(0), \mathbf{D}^T(1), \ldots, \mathbf{D}^T(N-1)]^T; \\ \mathbf{X}_k = [\mathbf{X}_k^T(0), \mathbf{X}_k^T(1), \ldots, \mathbf{X}_k^T(N-1)]^T; \\ k = 0,1,\ldots,K; \end{cases} \tag{9}$$

where $(\cdots)^T$ means a transpose. Equation (8) can be more compactly written as

$$\begin{cases} H_0: \quad \mathbf{X}_0 = \mathbf{D}, \\ H_1: \quad \mathbf{X}_0 = \alpha\mathbf{S} + \mathbf{D}. \end{cases} \tag{10}$$

The composite hypothesis testing problem (8) or (10) is also a two-sided parameter testing problem that tests $\alpha = 0$ against $\alpha \neq 0$. The general assumptions are the following:

1. The signal vector $\mathbf{S}$ is deterministic and known to the detector.
2. The signal amplitude α is complex valued, deterministic, and unknown.
3. The secondary data $\{\mathbf{X}_k\}_{k=1}^K$ and the disturbance signal $\mathbf{D}$, equivalently $\mathbf{X}_0$ under the hypothesis H_0 are i.i.d. with distribution $CN(\mathbf{0}, \mathbf{R})$, where $\mathbf{R}$ is the unknown space-time covariance matrix.

In particular, the above signal detection problem occurs in airborne space-time adaptive processing radar system with J array channels and coherent processing interval (CPI) of N pulse repetition intervals (PRIs). The disturbance $\mathbf{D}(n)$ consists of ground clutter, jamming, and thermal noise, while $\mathbf{S}(n)$ is the target space-time steering vector.

For a uniform equispaced linear array, the steering vector is [38]

$$\mathbf{S}(\omega_S, \omega_D) = \mathbf{S}_t(\omega_D) \otimes \mathbf{S}_S(\omega_S), \tag{11}$$

where $\mathbf{S}_S(\omega_S)$ denotes the $J \times 1$ spatial steering vector:

$$\mathbf{S}_S(\omega_S) = \frac{1}{\sqrt{J}}[1, \exp\{j\omega_S\}, \ldots, \exp\{j\omega_S(J-1)\}]^T \tag{12}$$

and $\mathbf{S}_t(\omega_D)$ denotes the $N \times 1$ temporal steering vector:

$$\mathbf{S}_t(\omega_D) = \frac{1}{\sqrt{N}}[1, \exp\{j\omega_D\}, \ldots, \exp\{j\omega_D(N-1)\}]^T, \tag{13}$$

where ω_S and ω_D denote the normalized target spatial and Doppler frequencies, respectively.

While the previous assumptions 1) – 3) are standard, we further assume that

4. The disturbance signal $\mathbf{D}(n)$ can be modelled as a multichannel AR(P) process with known model order P but unknown AR coefficient matrices and spatial covariance.

Additional comments on this assumption are the following. We clarify that our goal here is not to justify whether AR models are appropriate or not for the space-time adaptive processing applications.

As was shown in [38], the low-order multichannel AR models are very powerful and efficient in capturing the temporal and spatial correlation of the disturbance and, hence, can greatly help signal detection in airborne space-time adaptive processing systems. Our problem is how to exploit such a parametric model for the GD to solve the composite testing problem. The assumption that the model order P is known only used to simplify our presentation.

In practice, the model order selection techniques, such as the Akaike information criterion (AIC) and the minimum description length (MDL) based techniques [46] are available for this task. Since such techniques may overestimate or underestimate the true model order, a relevant problem is how the proposed detector performs when overestimation or underestimation occurs [47].

Finally, it is also possible to formulate the problem to include P as another parameter to be estimated. We do not follow such an approach in order to focus on the relations between the parametric Rao/GD test and the PAMF detector, which also assumes that a priori estimate of P is available. Based on this assumption, the secondary data $\{\mathbf{X}_k\}_{k=1}^K$ are represented as

$$\mathbf{X}_k(n) = -\sum_{p=1}^{P} \mathbf{A}^H(p)\mathbf{X}_k(n-p) + \varepsilon_k(n), \quad k = 1,2,\ldots,K, \tag{14}$$

where $\{\mathbf{A}^H(p)\}_{p=1}^P$ denote the $J \times J$ coefficient matrices, $(\cdots)^H$ denotes complex conjugate transpose, and $\varepsilon_k(n)$ denote the driving multichannel spatial noise vectors that are temporally white but spatially coloured Gaussian noise

$$\varepsilon_k(n) \cong CN\ (\mathbf{0},\mathbf{Q})\ , \tag{15}$$

where $\mathbf{Q}$ denotes the $J \times J$ signal covariance matrix.

Meanwhile, the test signal $\mathbf{X}_0$ is given by

$$\mathbf{X}_0(n) - \alpha\mathbf{S}(n) = -\sum_{p=1}^{P}\mathbf{A}^H(p)\{\mathbf{X}_0(n-p) - \alpha\mathbf{S}(n-p)\} + \varepsilon_0(n)\ , \tag{16}$$

where $\alpha = 0$ under the hypothesis H_0; $\alpha \neq 0$ under the hypothesis H_1, and

$$\varepsilon_0(n) \cong CN\ (\mathbf{0},\mathbf{Q})\ . \tag{17}$$

Let $\tilde{\mathbf{S}}(n)$ is a regression on $\mathbf{S}(n)$ and $\tilde{\mathbf{X}}_0(n)$ is a regression on $\mathbf{X}_0(n)$ under the hypothesis H_1:

$$\tilde{\mathbf{S}}(n) = \mathbf{S}(n) + \sum_{p=1}^{P}\mathbf{A}^H(p)\mathbf{S}(n-p)\ ; \tag{18}$$

$$\tilde{\mathbf{X}}_0(n) = \mathbf{X}_0(n) + \sum_{p=1}^{P}\mathbf{A}^H(p)\mathbf{X}_0(n-p)\ . \tag{19}$$

Then, the driving noise in (16) can be alternatively expressed as

$$\varepsilon_0(n) = \tilde{\mathbf{X}}_0(n) - \alpha\tilde{\mathbf{S}}(n)\ . \tag{20}$$

The problem of interest is to develop a decision rule for the above composite hypothesis testing problem using the test and training signals, as well as exploiting the multichannel parametric AR model.

4 A Priori Solutions

The number of solutions to the above problem has been developed. If the space-time covariance matrix $\mathbf{R}$ is known exactly, the MF statistic takes the following form [12]:

$$MF^{\text{out}} = \frac{|\mathbf{S}^H\mathbf{R}^{-1}\mathbf{X}_0|^2}{\mathbf{S}^H\mathbf{R}^{-1}\mathbf{S}} \underset{<_{H_0}}{\overset{>^{H_1}}{}} K_{MF}\ , \tag{21}$$

where K_{MF} denotes the MF threshold. The MF detector is obtained by a GLRT approach [7], by which the ML estimate of the unknown amplitude α is first estimated and then substituted back into the likelihood ratio to form a test statistic. It should be that the *MF* cannot be implemented in real applications since $\mathbf{R}$ is unknown. However, it provides a baseline for performance comparison when considering any realizable detection scheme.

In practice, the unknown $\mathbf{R}$ can be replaced by some estimate, such as the sample covariance matrix obtained from the secondary data:

$$\hat{\mathbf{R}} = \frac{1}{K}\sum_{k=1}^{K}\mathbf{X}_k\mathbf{X}_k^H\ . \tag{22}$$

Using $\hat{\mathbf{R}}$ in (21) leads us to the so-called AMF

$$AMF^{\text{out}} = \frac{|\mathbf{S}^H\hat{\mathbf{R}}^{-1}\mathbf{X}_0|^2}{\mathbf{S}^H\hat{\mathbf{R}}^{-1}\mathbf{S}} \underset{<_{H_0}}{\overset{>^{H_1}}{}} K_{AMF}\ , \tag{23}$$

where K_{AMF} is the AMF threshold [10]–[12]. Alternatively, one can treat both α and $\mathbf{R}$ as unknown and estimate them successively by ML.

Such a GLRT approach was pursued by Kelly [9], which gives the following Kelly test:

$$KELLY^{\text{out}} = \frac{|\mathbf{S}^H\hat{\mathbf{R}}^{-1}\mathbf{X}_0|^2}{[\mathbf{S}^H\hat{\mathbf{R}}^{-1}\mathbf{S}][K + \mathbf{X}_0^H\hat{\mathbf{R}}^{-1}\mathbf{X}_0]} \underset{<_{H_0}}{\overset{>^{H_1}}{}} K_{KELLY}\ , \tag{24}$$

where K_{KELLY} is the corresponding threshold. The AMF and KELLY tests are both *CFAR* detectors, what is desirable property in radar systems. However, they also entail a large training requirement. In particular, the sample covariance matrix $\hat{\mathbf{R}}$ has to be inverted, which imposes a constraint on the training size

$$K \geq JN \tag{25}$$

to ensure a full-rank $\hat{\mathbf{R}}$. The Reed-Brennan rule [8] suggests that at least $K \geq (2JN - 3)$ target-free secondary data vectors are needed to obtain the expected performance within 3 dB from the optimum MF. Such a training requirement may be difficult to meet, especially in nonhomogeneous or dense-target environments.

Besides excessive training, the computational complexity of these detectors is also high, since $\hat{\mathbf{R}}$ has to be computed and inverted for each CPI. While the AMF and KELLY tests may be called covariance matrix based techniques as they both involve computing and inverting $\hat{\mathbf{R}}$, the PAMF detector [38] utilize a multichannel AR(*P*) model that allows spatial/temporal whitening to be implemented in a multichannel time-series fashion

$$PAMF^{\text{out}} = \frac{\left|\sum_{n=P}^{N-1}\hat{\tilde{\mathbf{S}}}_P^H(n)\hat{\mathbf{Q}}_P^{-1}\hat{\tilde{\mathbf{X}}}_{0,P}(n)\right|^2}{\sum_{n=P}^{N-1}\hat{\tilde{\mathbf{S}}}_P^H(n)\hat{\mathbf{Q}}_P^{-1}\hat{\tilde{\mathbf{S}}}_P(n)} \underset{<_{H_0}}{\overset{>^{H_1}}{}} K_{PAMF}\ , \tag{26}$$

where $\hat{\mathbf{Q}}_P$ denotes an estimate of the spatial covariance matrix $\mathbf{Q}$, $\hat{\tilde{\mathbf{X}}}_{0,P}(n)$ and $\hat{\tilde{\mathbf{S}}}_P(n)$ are the temporally

whitened test signal and steering vector, respectively; these are whitened using an inverse AR(P) filter, i.e. multichannel MA filter whose parameters along with $\hat{\mathbf{Q}}_P$ are estimated from the secondary data. In contrast to simultaneous spatio-temporal whitening used in the AMF and KELLY tests, the PAMF detector performs whitening in two distinct steps: temporal whitening followed by spatial whitening.

The parametric approach offers savings in both training and computation, since the parameters to be estimated are significantly fewer, compared with covariance matrix based approaches. Applying the above principles to the case of parametric GD [23], [24] according to the generalized approach to signal processing in noise [18], [20], we have

$$GD^{\text{out}} = \frac{\left| 2\sum_{n=P}^{N-1} \hat{\tilde{\mathbf{S}}}_P^H(n)\hat{\mathbf{Q}}_P^{-1}\hat{\tilde{\mathbf{X}}}_{0,P}(n) - \sum_{n=P}^{N-1} \hat{\tilde{\mathbf{S}}}_P^H(n)\hat{\mathbf{Q}}_P^{-1}\hat{\tilde{\mathbf{S}}}_P(n) + \sum_{n=P}^{N-1} \mathbf{Q}_P^H\hat{\mathbf{Q}}_P^{-1}\mathbf{Q}_P \right|}{\sum_{n=P}^{N-1} \hat{\tilde{\mathbf{S}}}_P^H(n)\hat{\mathbf{Q}}_P^{-1}\hat{\tilde{\mathbf{S}}}_P(n)} \underset{<H_0}{\overset{>H_1}{}} K_{GD} \ . \quad (27)$$

5 Parametric Rao/GD Test

5.1 Test statistics

Parametric Rao/GD test with based on ML estimates of the nuisance parameters, i.e. parameters associated with the disturbance signal based on discussion in [2] is given by

$$Rao/GD^{\text{out}} = \frac{\left| 4\sum_{n=P}^{N-1} \hat{\tilde{\mathbf{S}}}^H(n)\hat{\mathbf{Q}}^{-1}\hat{\tilde{\mathbf{X}}}_0(n) - \sum_{n=P}^{N-1} \hat{\tilde{\mathbf{S}}}^H(n)\hat{\mathbf{Q}}^{-1}\hat{\tilde{\mathbf{S}}}(n) + \sum_{n=P}^{N-1} \mathbf{Q}^H\hat{\mathbf{Q}}^{-1}\mathbf{Q} \right|}{\sum_{n=P}^{N-1} \hat{\tilde{\mathbf{S}}}^H(n)\hat{\mathbf{Q}}^{-1}\hat{\tilde{\mathbf{S}}}(n)} \underset{<H_0}{\overset{>H_1}{}} K_{Rao/GD} \ , \quad (28)$$

where $K_{Rao/GD}$ is the test threshold that can be set by using the results in Subsection 5.2, $\hat{\tilde{\mathbf{S}}}(n)$ and $\hat{\tilde{\mathbf{X}}}_0(n)$ denote, respectively the steering vector and test signal that have been whitened temporally, and additional spatial whitening is provided by $\hat{\mathbf{Q}}^{-1}$ that is the inverse of the ML estimate of the spatial covariance matrix to be specified next.

Specifically, the temporally whitened steering vector and test signal in (28) are obtained as follows

$$\hat{\tilde{\mathbf{S}}}(n) = \mathbf{S}(n) + \sum_{p=1}^{P} \hat{\mathbf{A}}^H(p)\mathbf{S}(n-p) \ ; \quad (29)$$

$$\hat{\tilde{\mathbf{X}}}_0(n) = \mathbf{X}_0(n) + \sum_{p=1}^{P} \hat{\mathbf{A}}^H(p)\mathbf{X}_0(n-p) \ , \quad (30)$$

where $\hat{\mathbf{A}}^H(p)$ is the ML estimate of the AR coefficient matrix $\mathbf{A}^H(p)$.

To present the ML estimates more compactly, let

$$\mathbf{A}^H = [\mathbf{A}^H(1), \mathbf{A}^H(2), \ldots, \mathbf{A}^H(P)] \in C^{J \times JP} \quad (31)$$

which contains all the coefficient matrices involved in the P-th order AR model, and

$$\mathbf{Y}_k(n) = [\mathbf{X}_k^T(n-1), \mathbf{X}_k^T(n-2), \ldots, \mathbf{X}_k^T(n-P)]^T \ , \quad k = 0,1,\ldots,K \ , \quad (32)$$

which contains the regression subvectors formed from the test signal $\mathbf{X}_0$ or the k-th training signal $\mathbf{X}_k$.

We first compute the following correlation matrices:

$$\hat{\mathbf{R}}_{XX} = \sum_{n=P}^{N-1}\sum_{k=0}^{K} \mathbf{X}_k(n)\mathbf{X}_k^H(n) \ ; \quad (33)$$

$$\hat{\mathbf{R}}_{YY} = \sum_{n=P}^{N-1}\sum_{k=0}^{K} \mathbf{Y}_k(n)\mathbf{Y}_k^H(n) \ ; \quad (34)$$

$$\hat{\mathbf{R}}_{YX} = \sum_{n=P}^{N-1}\sum_{k=0}^{K} \mathbf{Y}_k(n)\mathbf{X}_k^H(n) \ . \quad (35)$$

Then, the ML estimates of the AR coefficients $\mathbf{A}^H$ and the spatial covariance matrix $\mathbf{Q}$ are given by

$$\hat{\mathbf{A}}^H = -\hat{\mathbf{R}}_{YX}^H\hat{\mathbf{R}}_{YY}^{-1} \ ; \quad (36)$$

$$\hat{\mathbf{Q}} = \frac{1}{(K+1)(N-P)}[\hat{\mathbf{R}}_{XX} - \hat{\mathbf{R}}_{YX}^H\hat{\mathbf{R}}_{YY}^{-1}\hat{\mathbf{R}}_{YX} \ . \quad (37)$$

The PGD also involves estimating the AR coefficients $\mathbf{A}^H$ and the spatial covariance matrix $\mathbf{Q}$. Several estimators were suggested including the Strand-Nuttall algorithm and the least-squares (LS) estimators. The LS estimator was observed to yield the better performance. Our ML estimator is similar to the LS estimator except that we use both the test and training signals to obtain the parameter estimates, whereas the latter utilizes only the training signals for parameter estimation. The subscript "P" is therefore used for the parameter estimates in (28) to indicate the difference.

Note that with the ML estimator, it is possible to derive the parameter estimates exclusively from the test signal, thus obviating the need for training. This could be advantageous where it is difficult to obtain

training signals that are i.i.d. with respect to the disturbance in the test signal.

The detection performance of the parametric Rao /GD in the absence of training signals will be explored elsewhere. We would like to point out that this approach is similar to Kelly's GLRT [9] which also employs both the test and the training signals for the parameter estimation. However, we stress that Kelly's GLR*T* does not exploit the multichannel parametric model as shown in (14) and (16). By comparing the parametric Rao/GD (28) and PGD test statistic (26), we can quickly see that if both detectors use the ML estimator for parameter estimation, they are identical except for a scaling factor of 2.

Hence, under the conditions stated in Section 3, the PGD is a parametric Rao/GD. It should be noted that similar to other space-time adaptive processing detectors, the parametric Rao/GD test is adaptive in that the detector is the data dependent detector, for example, the correlator. This shall not be confused with recursive adaptive implementation. Although a recursive adaptive implementation of the parametric Rao/GD test would be of interest in a real-time system, it is beyond the scope of the current paper.

5.2 Asymptotic analysis

The asymptotic distribution of the Rao/GD test statistic can be presented in the following form [20]

$$Rao/GD^{\text{out}} \overset{\alpha}{\cong} \begin{cases} H_0 \Rightarrow \chi_2^2; \\ H_1 \Rightarrow \chi_2'^2(\lambda), \end{cases} \tag{38}$$

where χ_2^2 is the central Chi-squared distribution with 2 degrees of freedom and $\chi_2'^2(\lambda)$ is the noncentral Chi-squared distribution with 2 degrees of freedom and noncentrality parameter λ:

$$\lambda = 2|\alpha|^2 \sum_{n=P}^{N-1} \tilde{\mathbf{S}}^H(n)\mathbf{Q}^{-1}\tilde{\mathbf{S}}(n) , \tag{39}$$

where $\tilde{\mathbf{S}}(n)$ is the temporally whitened steering vector given by (18).

Note that the value of λ is related to the SINR at the output of the temporal whitening filter. Recall that χ_2^2 random variable with probability density function (pdf) is given by

$$f_{\chi_2^2}(x) = \frac{1}{2}\exp\{-0.5x\}, \quad x \geq 0. \tag{40}$$

The pdf of $\chi_2'^2(\lambda)$ is given by [7]

$$f_{\chi_2'^2(\lambda)}(x) = \frac{1}{2}\exp\{-0.5(x+\lambda)\}I_0\left(\sqrt{\lambda x}\right), \quad x \geq 0 \tag{41}$$

where $I_0(u)$ is the modified Bessel function of the first kind and zero order defined by

$$I_0(u) = \frac{1}{\pi}\int_0^{\pi}\exp\{u\cos\theta\}d\theta = \sum_{k=0}^{\infty}\frac{[0.25u^2]^k}{(k!)^2} . \tag{42}$$

The above distributions can be employed to set the Rao/GD test threshold for the given probability of false alarm P_{FA}, as well as to compute the probability of detection P_D. For a given threshold, the probability of false alarm P_{FA} is given by

$$P_{FA} = \int_{K_{Rao/GD}}^{\infty} f_{\chi_2^2}(x)dx = \exp\{-0.5K_{Rao/GD}\}. \tag{43}$$

That can easily be inverted to find the test threshold $K_{Rao/GD}$ for the given probability of false alarm P_{FA}.

In addition, the probability of detection P_D is given by

$$P_D = \int_{K_{Rao/GD}}^{\infty} f_{\chi_2'^2}(x)dx$$

$$= \int_{K_{Rao/GD}}^{\infty} \frac{1}{2}\exp\{-0.5(x+\lambda)\}I_0\left(\sqrt{\lambda x}\right)dx \tag{44}$$

for the given test threshold $K_{Rao/GD}$.

The asymptotic distribution under the hypothesis H_0 is independent of the unknown parameters. The probability of false alarm P_{FA} in (43) depends only on the test threshold, which is a design parameter. It is evident that the Rao/GD test asymptotically achieves GD.

The above analysis holds under assumptions 1)–4) of Section 3 with one exception. In particular, since the ML parameter estimates are asymptotically Gaussian irrespective of the distribution of the observed data, the above analysis still holds if the Gaussian assumption in 3) is dropped. This statement also explains why it has been observed in several studies that the PGD obtains a good performance even under the non-Gaussian observations.

6 Performance of MF and AMF Detectors

Consider the MF detector (21) first. Let $\mathbf{R}^{-0.5}$ be the square root of the space-time covariance matrix $\mathbf{R}$. Define $\tilde{\mathbf{S}} = \mathbf{R}^{-0.5}\mathbf{S}$ and $\tilde{\mathbf{X}}_0 = \mathbf{R}^{-0.5}\mathbf{X}_0$ that are the spatially and temporally whitened steering vector and

the test signal, respectively. Since the rank of $\tilde{\mathbf{S}}\tilde{\mathbf{S}}^H$ is one, we have the following Eigen decomposition:

$$\tilde{\mathbf{S}}\tilde{\mathbf{S}}^H = \mathbf{U}\mathbf{B}\mathbf{U}^H, \quad (45)$$

where

$$\mathbf{B} = diag\{\tilde{\mathbf{S}}^H\tilde{\mathbf{S}},0,\ldots,0\} \text{ and } \mathbf{U}\mathbf{U}^H = \mathbf{I}. \quad (46)$$

Let

$$\overline{\mathbf{X}}_0 = \mathbf{U}^H\tilde{\mathbf{X}}_0 \text{ and } \overline{\mathbf{S}} = \mathbf{U}^H\tilde{\mathbf{S}}, \quad (47)$$

which are rotated versions of $\tilde{\mathbf{X}}_0$ and $\tilde{\mathbf{S}}$, respectively.

The test statistic can be defined as

$$MF^{\text{out}} = \frac{|\tilde{\mathbf{S}}^H\tilde{\mathbf{X}}_0|^2}{\tilde{\mathbf{S}}^H\tilde{\mathbf{S}}} = \frac{\tilde{\mathbf{X}}_0^H\mathbf{U}\mathbf{B}\mathbf{U}^H\tilde{\mathbf{X}}_0}{\tilde{\mathbf{S}}^H\tilde{\mathbf{S}}}$$

$$= \overline{X}_{0,1}^*\overline{X}_{0,1} = |\overline{X}_{0,1}|^2, \quad (48)$$

where $\overline{X}_{0,1}$ and $\overline{S}_1$ are the first element of $\overline{\mathbf{X}}_0$ and $\overline{\mathbf{S}}$, respectively, and $(\cdots)^*$ means the complex conjugate.

It is clear from assumptions 1–3 presented in Section 3 that $\overline{X}_{0,1}$ is a complex Gaussian variable:

$$\overline{X}_{0,1} \sim CN\ (\alpha\overline{S}_1, 1) \quad (49)$$

with $\alpha = 0$ under the hypothesis H_0 and $\alpha \neq 0$ under the hypothesis H_1. Hence, (48) is subjected to the central Chi-squared distribution with 2 degrees of freedom under the hypothesis H_0 and, respectively, the noncentral Chi-squared distribution with 2 degrees of freedom and the noncentrality parameter

$$\lambda_{MF} = 2|\alpha\overline{S}_1|^2 \quad (50)$$

under the hypothesis H_1.

It is noted that the distribution of the PAMF test statistic is similar to that of the parametric Rao/GD test statistic with the only difference of the noncentrality parameter under the hypothesis H_1. Hence, the probability of false alarm P_{FA} and the probability of detection P_D can be similarly computed as in (43) and (44).

The performance of the AMF detector (23) was analyzed in [12] that is summarized below. The density of a loss factor ρ defined in [12] is given by

$$f(\rho) = f_\beta(\rho; L-1, JN-1), \quad (51)$$

where $L = K - JN + 1$ and the central Beta density function is

$$f_\beta(x; n, m) = \frac{(n+m-1)!}{(n-1)!(m-1)!}x^{n-1}(1-x)^{m-1}. \quad (52)$$

The probability of false alarm P_{FA} is given by

$$P_{FA}^{AMF} = \int_0^1 \frac{f(\rho) = f_\beta(\rho; L-1, JN-1)}{(1+\eta\rho)^L}d\rho; \quad (53)$$

$$\eta = \frac{K_{KELLY}}{1-K_{KELLY}} \quad (54)$$

is the test threshold of Kelly's GLRT (24). Meanwhile, the probability of detection P_D is given by

$$P_D^{AMF} = 1 - \int_0^1 \frac{1}{(1+\eta\rho)^L}\sum_{m=1}^{L}\binom{L}{m}(\eta\rho)^m G_m\left(\frac{\xi\rho}{1+\eta\rho}\right)f(\rho)\,d\rho, \quad (55)$$

where

$$\xi = \mathbf{S}^H\mathbf{R}^{-1}\mathbf{S} \quad (56)$$

and $G_m(\cdots)$ is the incomplete Gamma function given by

$$G_m(y) = \exp\{-y\}\sum_{k=0}^{m-1}\frac{y^k}{k!}. \quad (57)$$

The integrals can be computed by numerical integration.

7 Simulation Results

In the following, we present our numerical results of the parametric Rao/GD obtained by computer simulation and by the above asymptotic analysis. In addition, the performance of the PAMF (24) and AMF (21) detectors that can be computed analytically, is included for comparison.

The disturbance signal is generated as a multichannel AR(2) process with randomly generated AR coefficients **A** and a spatial covariance matrix **Q**. In particular, **A** and **Q** are selected to ensure that **Q** is a valid covariance matrix and **A** is chosen to ensure that the resulting AR process is stable. Once **A** and **Q** are selected, they are fixed in all trials. The signal vector **S** is generated as in (9) with randomly chosen normalized spatial and Doppler frequencies.

The SINR is defined in the following form

$$SINR = |\alpha|^2\ \mathbf{S}^H\mathbf{R}^{-1}\mathbf{S}, \quad (51)$$

where **R** is the $JN \times JN$ joint space-time covariance matrix of the disturbance **D**, which can be determinied once **A** and **Q** are selected.

To numerically set the threshold for the parametric Rao/GD, a total of 5×10^4 trials has been run. Meanwhile, to determine the probability of detection P_D for a given threshold a total of 10^4 trials has been run for each SINR. We examine the receiver opera-

ting characteristic (ROC) of the parametric Rao/GD. The parameters used in the simulation are $J = 4$, $N = 32$ and $K = 256$.

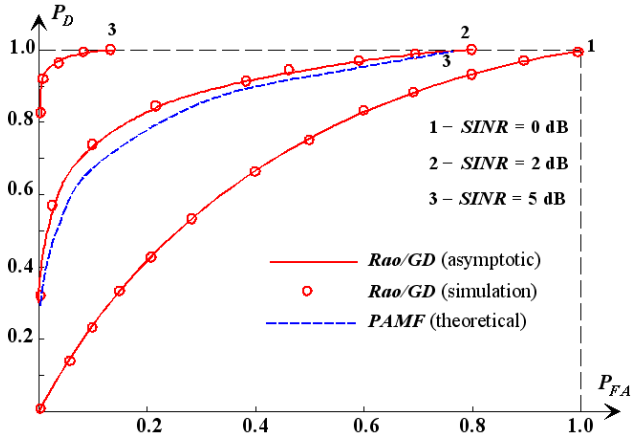

Figure 2. ROC curves.

Figure 2 depicts the ROC curves for the parametric Rao/GD obtained by simulation and asymptotic analysis for SINR values of 0, 2, and 5 dB. It is seen that the simulation results match those obtained by asymptotic analysis. The PAMF ROC is also presented for comparison. The superiority of the parametric Rao/GD over the PAMF is evident.

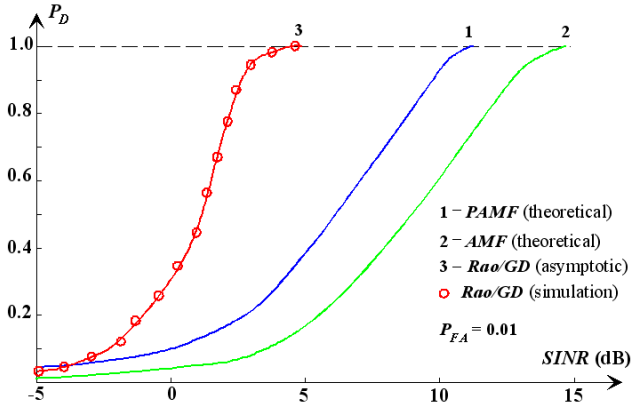

Figure 3. Probability of detection versus input *SINR* $J = 4,\ N = 32,\ K = 256$.

Figures 3–6 depict the probability of detection P_D versus SINR for the PAMF, AMF, and the parametric Rao/GD under various conditions. In particular, Figs. 3 and 5 correspond to the case with adequate training, for which the Reed-Brennan rule is satisfied, whereas Figs. 4 and 6 correspond to the case with limited training, for which the AMF detector does not even exist, since the training size $K = 8$ is too small to meet the minimum training condition (23).

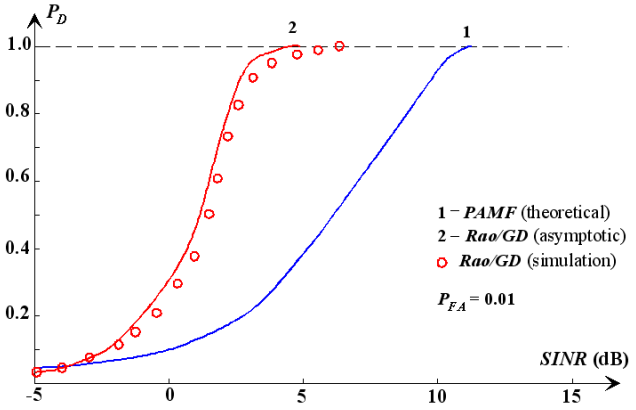

Figure 4. Probability of detection versus input *SINR* $J = 4,\ N = 32,\ K = 8$.

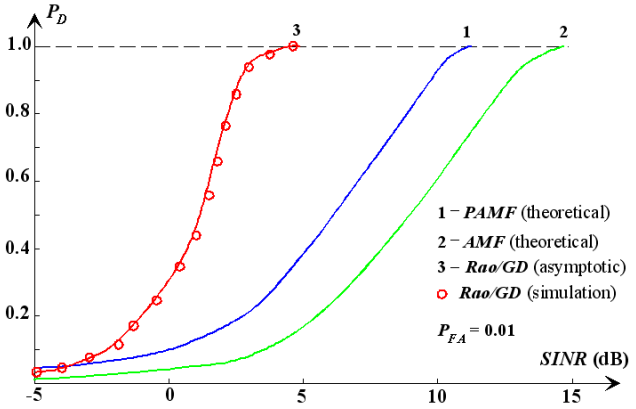

Figure 5. Probability of detection versus input *SINR* $J = 4,\ N = 16,\ K = 128$.

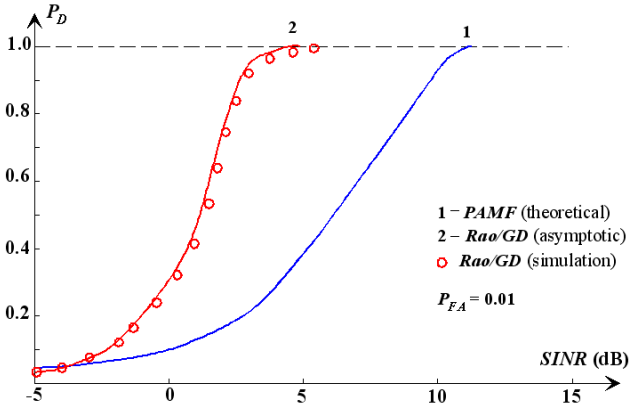

Figure 6. Probability of detection versus input *SINR* $J = 4,\ N = 16,\ K = 8$.

An examination of these figures reveals the following:

- When the assumptions of Section 3 are met, the asymptotic analysis provides a quite accurate prediction of the performance of the parametric Rao/GD. The gap between the asymptotic and simulated results is seen to widen as K and/or N

decreases. But even for the most challenging case with $K = 8$ and $N = 16$, the gap is about 0.5 dB, Fig.6;

- The parametric Rao/GD is very close to the theoretical GD. The gap between two detectors closes with increasing K and/or N;
- The parametric Rao/GD outperforms the PAMF and AMF detectors. So far we have assumed that the model order P of the multichannel AR process is known.

As mentioned, the various model selection techniques can be used to estimate P, and it is not unusual for these techniques to underestimate or overestimate the model order by a small number relative to the true model order P [46], [47].

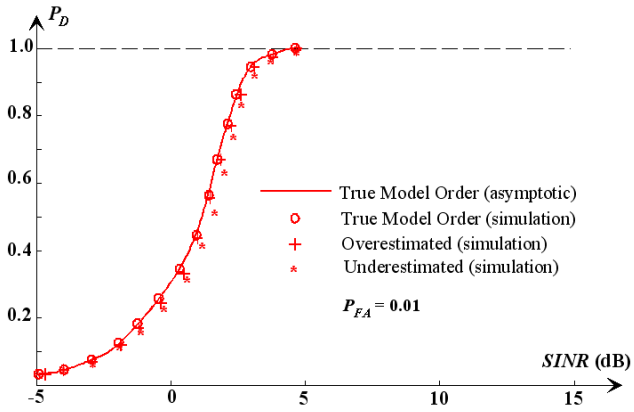

Figure 7. Probability of detection versus input *SINR* of parametric Rao/GD when model order of multichannel AR process used for computing test statistic is true ($P = 2$), underestimated (assuming $P = 1$), and overestimated (assuming $P = 3$,) along with $J = 4$, $N = 32$, $K = 256$.

It would be of interest to find out how the parametric Rao/GD performs when an inaccurate model order estimate is used. This is shown in Fig.7, where the performance of the Rao/GD using the true, an underestimated, and an overestimated model order is depicted. As we can see, using an inaccurate model order estimate degrades the detection performance, but the degradation is not significant, especially in the case of model order overestimation. Overestimation is a more robust error since the high-order coefficients can be estimated close to zero providing that the size of the signals that can be used for estimation is large enough.

The above behaviour of the parametric Rao/GD is typical and has been consistently observed in other experiments with a similar setup. Here, we only considered the case where the model order is inaccurately estimated by one unit. A larger performance variation is expected if there is a larger estimation error for P. Finally, Fig. 8 depicts the probability of detection P_D versus SINR for the parametric Rao/GD if $J = 4, P_{FA} = 0.01$ and N varies from $N = 4$ to $N = 128$. It is seen that the detection performance increases with N.

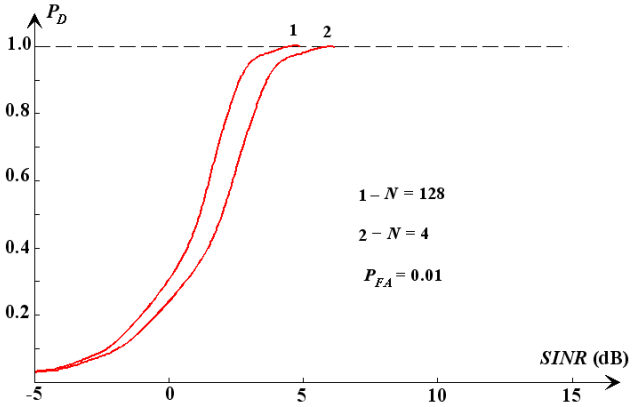

Figure 8. Impact of pulse number N on parametric Rao/*GD*.

8 Conclusions

We have developed a parametric Rao/GD test for the multichannel adaptive signal detection problem by exploiting a multichannel AR model. We have derived the ML estimates of the parameters involved in the test. The parametric Rao/GD test is asymptotic PGD, and the asymptotic distributions of its test statistic under both hypotheses have been obtained in the closed form. Computer simulations show that:

- Our asymptotic analysis provides fairly accurate prediction of the parametric Rao/GD test performance;
- Even with relatively limited training, the parametric Rao/GD is quite close to the ideal GD;
- The parametric Rao/GD outperforms the AMF detector, which does not exploit a parametric model;
- The performance of the parametric Rao/GD is affected by inaccurate model order estimation, but the resulting performance degradation is tolerable when the model order estimation error is small.

Our asymptotic analysis of the parametric Rao/GD is based on several assumptions in Section 3, including that the disturbance can be modeled as an AR(P) process with known model order P, and that the training signals are i.i.d. When these assumptions are violated, we expect that the analysis will be

less accurate, but may still be informative if the assumptions are not significantly violated. For example, we have noticed in simulation that when the disturbance is an MA process, the test threshold obtained by analysis assuming an AR model is still quite accurate.

One possible reason is that AR models are fairly general parametric models, and under mild conditions, can be used to model or approximate a large class of stationary random processes, for example, an MA process can be approximated as an AR process with a high enough model order [48]. Nevertheless, there is a need to find out how accurate our analysis is in real systems with real data, when assumptions of Section 3 may not all be met. This will be an interesting future effort.

Acknowledgment

This research was supported by Industry-Academic Cooperation Foundation, Kyungpook National University and SL Light Corporation Joint Research Grant (the Grant No. 201014590000) and the Kyungpook National University Research Grant, 2013.

References:

[1] Ward, J., "Space-time adaptive processing for airborne radar," Lincoln Laboratory, MIT, Techn. Report 1015, Dec. 1994

[2] Klemm, R., *Principles of Space-Time Adaptive Processing*. London, IEE Press, 2002.

[3] Shaw, G. and D. Manolakis, "Signal processing for hyperspectral image exploitation," *IEEE Signal Processing Magazine*, 2002, Vol.19, No.1, pp.12–16.

[4] Manolakis, D. and G. Shaw, "Detection algorithms for hyperspectral imaging applications," *IEEE Signal Processing Magazine*, 2002, Vol. 19, No.1, pp.29–43.

[5] Paulraj, A. and C.B. Papadias, "Space-time processing for wireless communications," *IEEE Signal Processing Magazine*,1997, Vol.14, No.11, pp.49–83.

[6] Justice, J.H., "Array processing in exploration seismology," in *Array Signal Processing*, Editor: Simon Haykin, Englewood Cliffs, NJ: Prentice-Hall, 1985.

[7] Kay, S.M., *Fundamentals of Statistical Signal Processing: Detection Theory*,Englewood Cliffs, NJ: Prentice-Hall, 1998.

[8] Reed, I.S., Mallet, J.D., and L.E Brennan, "Rapid convergence rate in adaptive arrays," *IEEE Transactions on Aerospace and Electronic Systems*, 1974, Vol.10, No.6, pp.853–863.

[9] Kelly, E.J., "An adaptive detection algorithm," *IEEE Transactions on Aerospace and Electronic Systems*, 1974, Vol.10, No.6, pp.115–127.

[10] Cai, L. and H. Wang, "On adaptive filtering with the CFAR feature and its performance sensitivity to non-Gaussian interference," in *Proceedings 24th Annual Conference on Information Sciences and Systems*, 1990, March, Princeton, NJ, USA, pp.558–563.

[11] Chen, W. and I.S., Reed, "A new CFAR detection test for radar," *Digital Signal Processing*, 1991, Vol.1, No.4, pp.198–214.

[12] Robey, F.C., Fuhrmann, D.R., Kelly, E.J., and R. Nitzberg, "A CFAR adaptive matched filter detector," *IEEE Transactions on Aerospace and Electronic Systems*, 1974, Vol.10, No.6, pp.115–127.

[13] Kraut, S. and L.L., Scharf, "The CFAR adaptive subspace detector is a scale-invariant GLRT," *IEEE Transactions on Signal Processing*, 1999, Vol.47, No.9,pp.2538–2541.

[14] Kraut, S., Scharf, L.L., and L.T. McWhorter, "Adaptive subspace detectors," *IEEE Transactions on Signal Processing*, 1999, Vol.47, No. 9, pp.2538–2541.

[15] Tuzlukov, V.P., "Adaptive generalized detector for unknown power spectral densities in noise," in *Proceedings International Signal Processing Conference*(*ISPC'03*), Dallas, TX, March 31–April 4, 2003.

[16] Tuzlukov, V.P., "Adaptive beamformer generalized detector in wireless sensor networks," in *Proceedings IASTED International Conference on Parallel and Distributed Computing and Networks* (*PDCN*), Rhodes Island, Greece, June 30–July 2, 2003.

[17] Kim, Y.D., Yoon, W.S., and V.P. Tuzlukov, "Adaptive beamformer generalized detector in wireless sensor networks," in *Proceedings IASTED International Conference on Parallel and Distributed Computing and Networks* (*PDCN 2004*), Innsbruck, Austria, February 17–19, 2004, pp.195– 200.

[18] Tuzlukov, V.P., "A new approach to signal detection theory," *Digital Signal Processing*, 1998, Vol. 8, No. 3, pp. 166–184.

[19] Tuzlukov, V.P., *Signal Processing in Noise*: *A New Methodology*, Minsk: IEC, 1998.

[20] Tuzlukov, V.P., *Signal Detection Theory*, New York: Springer-Verlag, 2001

[21] Tuzlukov, V.P., *Signal Processing Noise*, Boca Raton, London, New York, Washington D.C.: CRC Press, Taylor & Francis Group, 2002.

[22] Tuzlukov, V.P., *Signal and Image Processing in Navigational Systems*, Boca Raton, London, New York,Washington D.C.:CRC Press,Taylor

& Francis Group, 2005.
[23] Tuzlukov, V.P., *Signal Processing in Radar Systems*, Boca Raton, London, New York, Washington D.C. CRC Press, Taylor & Francis Group, 2012.
[24] Tuzlukov, V.P., "DS-CDMA downlink systems with fading channel employing the generalized receiver," *Digital Signal Processing*, 2011, Vol. 21, No. 6, pp.725–733.
[25] Tuzlukov, V.P., "Signal processing by generalized receiver in DS-CDMA wireless communication systems with frequency-selective channels," *Circuits, Systems, and Signal Processing*, 2011,Vol. 30, No. 6, pp.1197–1230.
[26] Tuzlukov, V.P., " Signal processing by generalized receiver in DS-CDMA wireless communication systems with optimal combining and partial cancellation," *EURASIP Journal on Advances in Signal Processing*, Vol. 2011, Article ID 913189, 15 pages, 2011, doi:10.1155/2011/913189.
[27] Tuzlukov, V.P. "Generalized approach to signal processing in wireless communications: the main aspects and some examples," Ch. 11 in *Wireless Communications and Networks: Recent Advances*. Editor: Eksim Ali, INTECH, Croatia, 2012, pp.305–338.
[28] Tuzlukov, V.P., "Wireless communications: generalized approach to signal processing," Ch. 6 in *Communication Systems: New Research*. Editor: Vyacheslav Tuzlukov, NOVA Science Publisher, Inc., New York, USA, 2013, pp.175 –268.
[29] Tuzlukov, V.P., "Signal processing by generalized receiver in DS-CDMA wireless communication Systems," Ch. 1 in *Wireless Communications*, Editor: Mutamed Khatib, INTECH, 2014.
[30] Shbat, M.S. and V.P. Tuzlukov, "Radar sensor detectors for vehicle safety systems," Chapter 1 in *Autonomous Hybrid Vehicles: Intelligent Transport Systems and Automotive Technologies*, Editors: Nicu Bizon, Lucian Dascalescu, and Naser Tabatabaei, Publishing House, University of Pitesti, Romania, 2013, pp. 1–27.
[31] Shbat, M.S. and V.P. Tuzlukov, "Radar sensor detectors for vehicle safety systems," Ch.1 in *Autonomous Vehicles: Intelligent Transport Systems and Smart Technologies*, Editors: Nicu Bizon, Lucian Dascalescu, and Naser Tabatabaei, Nova Science Publishers, Inc.,New York, 2014, pp.
[32] Shbat, M.S. and V.P. Tuzlukov, "Evaluation of detection performance under employment of generalized detector in radar sensor systems," *Radioengineering*, 2014, Vol. 23, No. 1, pp.50 –65.
[33] Shbat, M.S. and V.P. Tuzlukov, "Generalized detector with adaptive detection threshold for radar sensors," in *Proc. International Radar Symposium (IRS 2012)*, Warsaw, Poland, 2012, pp. 91–94.
[34] Shbat, M.S. and V.P. Tuzlukov, "Noise power estimation under generalized detector employment in automotive detection and tracking systems," in *Proc. 9th IET Data Fusion and Target Tracking Conf. (DF&TT'12)*, London, UK, 2012, doi: 10.1049/cp.2012.0416.
[35] Shbat, M.S. and V.P. Tuzlukov, "Definition of adaptive detection threshold under employment of the generalized detector in radar sensor systems," *IET Signal Processing*, 2014, Vol. 8, Issue 6, pp.622–632.
[36] Shbat, M.S. and V.P. Tuzlukov, "Spectrum sensing under correlated antenna array using generalized detector in cognitive radio systems," *International Journal of Antennas and Propagation*, vol. 2013, Article ID 853746, 8 pages, 2013, doi:10.1155/2013/853746.
[37] Rangaswamy, M. and J.H. Michels, "A parametric multichannel detection algorithm for correlated non-Gaussian random processes," in *Proceedings 1997 IEEE National Radar Conference*, Syravuse, NY,May 1997, pp.349–354.
[38] Roman, J.R, Rangaswamy, M., Davis, D.W., Zhang, Q., Himed, B., and J.H. Michels, "Parametric adaptive matched filter for airborne radar applications," *IEEE Transactions on Aertospace and Electronic Systems*, 2000, Vol.36, No.4, pp.677–692.
[39] Swindlehurst, A.I. and P. Stoica, "Maximum likelihood methods in radar array signal processing," *IEEE Proceedings*, 1998, Vol.86, No.2, pp.421–441.
[40] Li, J., Liu, G., Jiang, N., and P. Stoica, "Moving target feature extraction for airborne high-range resolution phased-array radar," *IEEE Transactions on Signal Processing*, 2001, Vol. 49, No.2, pp.277–289.
[41] Conte, E. and A. De Maio, "Distributed target detection in compound-Gaussian noise with Rao and Wald tests," *IEEE Transactions on Aerospace and Electronic Systems*, 2003, Vol. 39, No.4, pp.568–582.
[42] De Maio, A., Alfano, G., and E. Conte, "Polarization diversity detection in compound-Gaussian clutter," *IEEE Transactions on Aerospace and Electronic Systems*, 2003, Vol.39, No.4, pp.568–582.
[43] Maximov, M., "Joint correlation of fluctuative

noise at outputs of frequency filters," *Radio Eng*., No. 9, 1956, pp.28–38.

[44] Chernyak, Yu. "Joint correlation of noise voltage at outputs of amplifiers with nonoverlapping responses," *Radio Phys. and Elec*., No. 4, 1960, pp. 551–561.

[45] Shbat, M.S. "Performance analysis of signal detection by GD in radar sensor and cognitive radio systems," *Kyungpook National University, PhD Thesis*, 131 p., December 2013.

[46] Stoica, P. and Moses, R.L., *Spectral Analysis of Signals*, Englewood Cliffs, NJ: Prentice-Hall, 2005.

[47] Tsao, T., Himed, B., and J.H. Michels, "Effects of interference rank estimation on the detection performance of rank reduced STAP algorithm," in *Proceedings 1998 IEEE Radar Conference*, May 1998, pp.147–152.

[48] Kay, S.M., *Moder Spectral Estimation: Theory and Applications*, Englewood Cliffs, NJ: Prentice-Hall, 1988.